

Analysis of guided mode in TC-SAW device by using multi-mode COM model

マルチモード COM を用いた TC-SAW 導波モードの解析

Gongbin Tang¹, Rei Goto¹, and Hiroyuki Nakamura^{1†}

(¹Skyworks Solutions, Inc., Kadoma, Osaka 5710050, Japan)

唐 供賓^{1†}, 後藤 令¹, 中村 弘幸^{1†} (¹スカイワークスソリューションズ)

1. Summary

TC-SAW devices using SiO₂ film on LiNbO₃ have been widely employed in filters and duplexers for applications to the cellular handset market¹⁻⁴.

Usually, the coupling of modes (COM) model is employed for design and analysis of TC-SAW devices. However, with more and more stringent requirements on device performance, SH mode spurious is becoming a vital problem for Rayleigh type TC-SAW devices, due to the fact that it will not only introduce in-band spikes, but also deteriorate the passband insertion loss (IL). As a countermeasure, some researchers introduced a so-called multi-mode COM model. This model includes the mutual coupling between Rayleigh mode and SH mode, which is quite helpful for analysis and suppression of the spurious modes.

A lot of work has been done to suppress the SH spurious modes in the vicinity of the passband. However, for carrier aggregation (CA) applications, it is not enough to only consider the modes in vicinity of the passband, the guided mode, which is substantially confined to the SiO₂ film and has an interaction with the Rayleigh mode, which should also be analyzed and suppressed.

By referring to the development of multi-mode COM model used for SH mode analysis, this paper introduces how to analyze the guided mode in TC-SAW devices by using the same methodology.

2. Guided Mode in TC-SAW

A typical TC-SAW device is overcoated by SiO₂ overlayer on top of the IDT, sometimes named as buried interdigital transducer (BIDT)². Figure 1 illustrates a TC-SAW device stack configuration in sagittal plane, where 128°YX LiNbO₃ is employed as substrate. SiO₂ is deposited surrounding IDT to improve the temperature coefficient of frequency (TCF). Figure 2 shows a measured resonator admittance response with the guided mode influence. Two kinds of guided modes exist, one shows up ~1.3 times of the resonant frequency f_r and another one shows up ~1.8 times of f_r . For a better understanding of mode mechanisms, we show the corresponding total displacements in the insets of Fig.2, where commercial finite element method (FEM) software COMSOL is employed for the calculation. We can see both the two guided modes are due to energy concentration in the SiO₂

film. If filters or multiplexers are designed based on such resonators like shown in Fig.2, we will see filter transmission performance similar to that of Fig.3, where neighboring bands will be loaded by unexceptional loss.

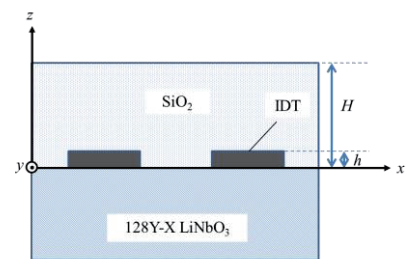


Fig. 1 TC-SAW device in sagittal plane

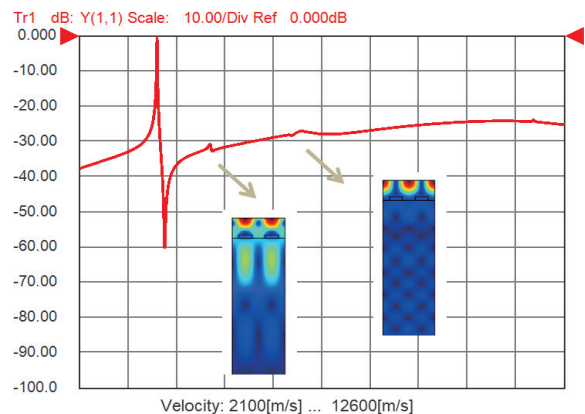


Fig. 2 Measured TC-SAW resonator admittance characteristics

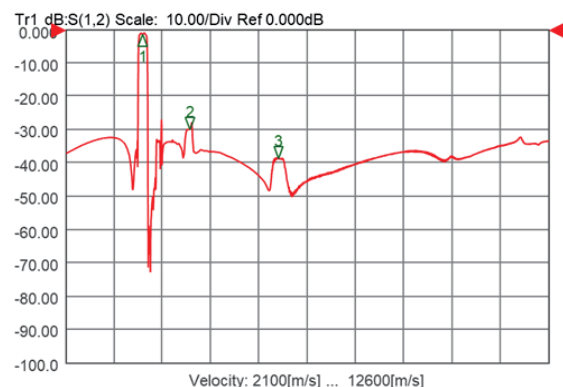


Fig. 3 Influence of guided mode on TC-SAW filter transmission characteristics

3. COM Model for Two Modes

We would like to adopt the same methodology as that used for SH and Rayleigh coupling case. As discussed by Goto³⁾, we employ the following wave equation for the discussion:

$$\begin{aligned} \frac{\partial U_1}{\partial x} &= -j\theta_{u1}U_1 + j\kappa_{12}U_2 + j\kappa_{13}U_3 + j\kappa_{14}U_4 + j\alpha_1 \\ \frac{\partial U_2}{\partial x} &= +j\kappa_{21}U_1 + j\theta_{u1}U_2 + j\kappa_{23}U_3 + j\kappa_{24}U_4 - j\alpha_1 \\ \frac{\partial U_3}{\partial x} &= +j\kappa_{31}U_1 + j\kappa_{32}U_2 - j\theta_{u2}U_3 + j\kappa_{34}U_4 + j\alpha_2 \\ \frac{\partial U_4}{\partial x} &= +j\kappa_{41}U_1 + j\kappa_{42}U_2 + j\kappa_{43}U_3 + j\theta_{u2}U_4 - j\alpha_2 \end{aligned} \quad (1)$$

where U_1 and U_2 correspond to the forward and backward propagating Rayleigh modes. U_3 and U_4 correspond to those of the SH modes. κ_{12} and κ_{21} are reflection coefficients for Rayleigh mode and κ_{34} and κ_{43} SH mode. Except those mentioned coefficients, remaining κ_{ij} stands for mutual coupling coefficients. Besides, α_1 and α_2 stands for the excitation coefficient of the Rayleigh mode and guided mode respectively.

Based on Fig.1 and parameters: $h=0.065\lambda$, $H=0.4\lambda$, where λ stands for the resonant wavelength, duty factor (DF) of IDT is 0.45, we extracted the general parameters from finite element method and spectral domain analysis (FEMSDA) as initial input of the multi-mode COM model. Figure 4 illustrates the calculated Brillouin dispersion diagram. As is well known, the mutual coupling between the Rayleigh mode and guided mode is much stronger than that between the Rayleigh mode and SH mode²⁾. Even so, we would like to enlarge the mutual coupling factor by 10 times for a better understanding.

There are two existing modes in Fig.4. As for the Rayleigh mode, its short-circuited (SC) dispersion branch, shown in blue line, and the open-circuited (OC) dispersion branch, shown in red line, are both located at the lower frequency side. To the contrary, the guided mode SC and OC branches are located at the higher frequency side. Further insight into Fig.4 shows the Rayleigh mode is resonating at the lower SC stopband edge, while the guided mode is resonating at the higher SC stopband edge. A stopband due to the strong interaction of the Rayleigh and guided mode branch forms in between the two modes. We will give more details on influence of this mutual coupling later⁴⁾.

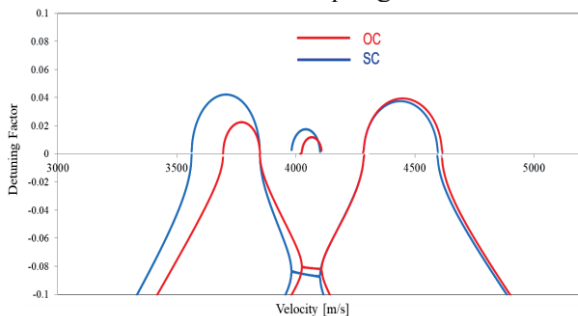


Fig. 4 Dispersion curve for guided mode and Rayleigh mode with mutual coupling

4. Experimental Verification

To validate the effectiveness of this model, we fabricated one port synchronous resonators on 128°YX-LN with the stack configuration shown in Fig. 1 and geometry parameters used in part 3. As shown in Fig. 5, although loss is not accurately matched, the multi-mode COM model can agree with the experimental result quite well. The disagreement around Rayleigh mode anti-resonant frequency f_a is due to SH mode responses and Rayleigh transverse modes, while the one after guided mode f_a is due to bulk radiation.

As we expected, the longitudinal ripples of the Rayleigh mode and the guided mode are located below/above the corresponding f_r , this verified the location of f_r is at the lower/upper SC stopband edge, for the two modes. It is interesting to note that when frequency is higher than the Rayleigh mode upper stopband edge, capacitance for the resonator changed, which may be caused by change of the electric field distribution.

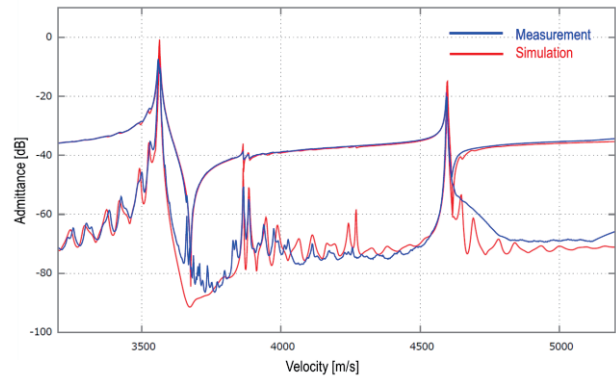


Fig. 5 Experimental verification of the multi-mode COM model for guided mode analysis

As a next step, we would like to apply this method to design of duplexers.

References

1. K. Yamanouchi, S. Hayama, IEEE Trans. on Sonics and Ultrason., SU-31, (1984) pp. 51-57.
2. B. Abbott, A. Chen, T. Daniel, K. Gamble, T. Kook, M. Solal, K. Steiner, R. Aigner, S. Malocha, C. Hella, M. Gallagher, and J. Kuypers, Proc. IEEE Ultrasonics (2017), p. 1.
3. R. Goto, J. Fujiwara, H. Nakamura, and K. Hashimoto, Jpn. J. Appl. Phys. 57, 07LD20 (2018).
4. Y. Huang, J. Bao, X. Li, B. Zhang, G. Tang, T. Omori, K. Hashimoto, IEEE transactions on Ultrasonics, Ferroelectrics, and Frequency Control, 65(10), (2018) 1905-1913.